

An Update to the NASA Reference Solar Sail Thrust Model

Andrew F. Heaton¹,
NASA Marshall Space Flight Center, AL, 35812

Alexandra B. Artusio-Glimpse²,
Rochester Institute of Technology, Rochester, NY, 14628

An optical model of solar sail material originally derived at JPL in 1978 has since served as the de facto standard for NASA and other solar sail researchers. The optical model includes terms for specular and diffuse reflection, thermal emission, and non-Lambertian diffuse reflection. The standard coefficients for these terms are based on tests of 2.5 micrometer Kapton sail material coated with 100 nm of aluminum on the front side and chromium on the back side. The original derivation of these coefficients was documented in an internal JPL technical memorandum that is no longer available. Additionally more recent optical testing has taken place and different materials have been used or are under consideration by various researchers for solar sails. Here, where possible, we re-derive the optical coefficients from the 1978 model and update them to accommodate newer test results and sail material. The source of the commonly used value for the front side non-Lambertian coefficient is not clear, so we investigate that coefficient in detail. Although this research is primarily designed to support the upcoming NASA NEA Scout and Lunar Flashlight solar sail missions, the results are also of interest to the wider solar sail community.

Nomenclature

A	= sail area
B_b, B_f	= back and front non-Lambertian coefficients, respectively
F_t	= tangential force component in the xy plane of the sail body
F_n	= normal force component along sail z body axis
P	= solar pressure at one astronomical unit (AU)
\tilde{r}	= reflection coefficient
s	= fraction of specular reflection coefficient
e_b, e_f	= back and front surface emissivity, respectively
D	= diffusivity
α	= sun incidence or pitch angle
AL	= aluminum
E_i	= irradiance on sail
P_i, P_r	= power of light impinging and reflecting off sail surface, respectively
σ	= surface area of a hemisphere
$d\omega$	= elementary solid angle of a reflected cone of light
θ	= angle of reflection of a ray
ϕ	= cone angle in the plane of the sail of a reflected ray
L_r	= radiance of reflected light off the sail
I_r	= radiant intensity of reflected light
$BRDF$	= Bi-directional Reflectance Distribution Function
c	= speed of light in vacuum
$\delta(\cdot)$	= Dirac delta function
$f_d(\theta, \phi)$	= distribution function of diffusely reflected light

¹ Senior Aerospace Engineer, EV42/Guidance, Navigation, and Mission Analysis, NASA Marshall Space Flight Center, Member AIAA

² PhD Candidate, Rochester Institute of Technology, National Science Foundation Fellow

I. Introduction

The current solar sail thrust model used as a reference for NASA for preliminary mission design studies is based on optical testing that occurred at JPL in 1978 in support of the (later canceled) solar sail mission to Halley's Comet [1]. The model was derived in an internal JPL memo that has since been lost, but it was later published in two standard reference texts for solar sails [2,3] and has since been used extensively in solar sail mission design and research [4-5]. This model consists of the following equations:

$$F_t = -PA(1 - \tilde{\mathbf{r}}\mathbf{s}) \cos(\alpha) \sin(\alpha) \quad (1)$$

$$F_n = -PA(1 - \tilde{\mathbf{r}}\mathbf{s}) \cos^2(\alpha) - PAB_f(1 - \mathbf{s})\tilde{\mathbf{r}} \cos(\alpha) - PA(1 - \tilde{\mathbf{r}})\left(\frac{\mathbf{e}_f\mathbf{B}_f - \mathbf{e}_b\mathbf{B}_b}{\mathbf{e}_f + \mathbf{e}_b}\right) \cos(\alpha) \quad (2)$$

The terms of equations (1) and (2) are defined in the nomenclature. The equations are derived in the body reference frame of the solar sail. Equation (1) represents what J. Wright and C. McInnes call the *tangential force*, or force in the plane of the sail, while Equation (2) describes the *normal force*, or force orthogonal to the plane of the sail. A perfectly flat solar sail is assumed in the derivation of these equations. In the literature by both Wright and McInnes, an additional clock angle orients the tangential force within the sail plane. Typically this angle is only needed for relating the sail force to an inertial or other external reference frame, and is not used in this paper since this paper is primarily concerned with reviewing and updating the coefficients in Equations (1) and (2), which depend only on the pitch angle α . The pitch angle is the angle between the incident light and the plane of the sail.

In this paper, we re-derive each coefficient from data in Ref. [1]. This re-derivation serves a two-fold purpose. One, it recreates (where possible) the original derivation of these coefficients for archival purposes, and two, it allows researchers to review the original assumptions made in that derivation for relevance and accuracy to recent and current solar sail projects. We then update these coefficients to support the NASA solar sail flight projects NEA Scout and Lunar Flashlight [7]. We discuss ongoing challenges, developments, and potential future work that could lead to continued improvements to the NASA solar sail reference thrust model.

II. Derivation of 1978 Coefficients

The coefficients derived for the Halley's Comet mission and published in Refs. [2,3] appear in Table 1.

Coefficient	$\tilde{\mathbf{r}}$	\mathbf{s}	\mathbf{B}_f	\mathbf{B}_b	\mathbf{e}_f	\mathbf{e}_b
Value	0.88	0.94	0.79	0.55	0.05	0.55

Table 1. Sail thrust model optical coefficients from Halley's Comet Solar Sail mission tests [2, 3]

In order to determine the origin of these coefficients, we extensively reviewed NASA report, NASA-CR-157870. In this section we attempt to re-derive each of the optical coefficients in Equations (1) and (2), from the most significant to the least significant, beginning with the total reflectance ($\tilde{\mathbf{r}}$).

The source of $\tilde{\mathbf{r}}$ is comes from the following quote found on page 4-30 of Ref. [1], where it states that reflectance values were measured "...in the range of 0.88 to 0.91. Based on these data, a criterion was established for a minimum spectral reflectance of 0.88 for aluminized coatings." The term "spectral" in this case is an indication that the measurement was weighted against the solar spectrum, which is a standard practice in determinations of solar reflectivity. So it can be seen that $\tilde{\mathbf{r}}$ was a conservative value from a range of measurements and the source of the 1978 value presented in Table 1 is straightforward.

The source of \mathbf{s} is not quite as straightforward, but we have determined that it comes from Table 4-6 in Ref. [1], which is reproduced below as Table 2. The original title of that table is also retained.

One can discover the source of the published value of \mathbf{s} in Table 1 by a close examination of Table 2. Table 2 lists the results of three measurements performed for a Bi-directional Reflectance Distribution Function (BRDF) test, which is a standard way of determining diffuse reflection of an opaque surface [8]. Specular reflection is light reflected at the incident angle of the light (see Fig. 1(a)). Diffusivity in the theoretical sense is light reflected at angles other than

the incident angle (see Fig. 1(b)). Generally diffusivity is defined in a more practical sense as light reflected outside a cone of a certain size around the incident angle. Listed in Table 2 are varying cone sizes that JPL selected for this particular diffusivity study. Although this assumption is not documented in Wright or McInnes, it has been stated [9] that the diffusivity values that appear in those books are based on a cone angle of 10 deg. This statement is confirmed by an analysis of Table 2.

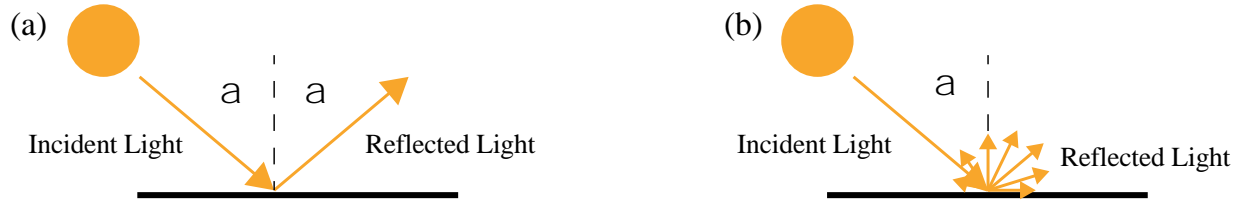


Figure 1. (a) Specular Reflection, and (b) Diffuse Reflection

Reflectometer Aperture	1 Inch Mask	1.12 Inch Mask	1.4 Inch Mask
Polar Angle of Specular Reflectometer Measurement (deg)	5.3 deg	8.5 deg	10.5 deg
Solar Reflectance	0.864	0.864	0.864
Diffuse Reflectance	0.227	0.098	0.035
Normalized Specular Reflectance	0.737	0.887	0.959

Table 2. Optical measurements of specular reflective properties of 100 nm AL-coated Kapton, reproduction of Table 4-6 from [1].

Called “Solar Reflectance” in Table 2, the values in row 2 are reflectance coefficients, denoted by \tilde{r} in Table 1, while “Diffuse Reflectance” is the raw measurement of diffusivity as determined by the BRDF. “Normalized Specular Reflectance” is the coefficient s we seek, and is given by

$$s = (1-D)/\tilde{r} \quad (3),$$

where D is the measured diffusivity of the surface. The value of s published in Refs. [2] and [3] that appears in Table 1 can be reproduced by a linear interpolation between the polar angle of the second row of Table 2 for 10 deg. Although the assumption of a 10 deg cone for the determination of diffusivity is not documented in those sources, it is clear from the interpolation of Table 2 that this was indeed the assumption, and that Table 2 (reproduction of Table 4-6 in [1]) is the source of this value.

Note also that the reflectivity characteristics measured above come from a front AL coated sail. Tests documented in [1] (and verified by more recent tests) indicate that 100 nm of AL is more than sufficient to ensure that the reflective characteristics of the sail will be those of AL and not the underlying substrate (whether that is Kapton, Mylar, CP1, or some other material). Fig. 4-10 in NASA report NASA-CR-157870 indicates that above ~ 40 nm of AL, transmission drops below 1%, and thus 100 nm is a significant margin to ensure that the underlying substrate does not contribute to reflective properties. The reflective properties of a sail coated with AL are, thus, determined by the AL and not by the underlying substrate for a sufficiently thick coating. This, however, is not the case for emissivity.

Emissivity is a strong function of not only the material composition of the underlying substrate, but also the thickness of the various coatings on the either side of the substrate. As previously stated, the numbers for front and back side emissivity published by Wright and McInnes are based on a 100 nm coating of AL on the front side and a chromium coating on the back side. The chromium strongly impacts the back side emissivity of the sail.

The value for the back side emissivity coefficient in Table 1 comes from Figure 4-16 of NASA report NASA-CR-157870. We have been unable to determine the source of the front side emissivity, but the value of 0.05 is in family with later measurements of 100 nm of AL coating a polymer substrate [10]. In any event, the source of the derivation

of emissivity coefficients is only of archival interest, since NEA Scout and Lunar Flashlight are using CP1 coated with 100 nm of AL on the front side and no coating on the back side, which thus has much different emissivity properties. In addition, emissivity has generally a much smaller effect than reflectivity with regard to solar sail thrust. Errors in emissivity coefficients are, therefore, less critical.

A non-Lambertian coefficient is designed to capture the deviation of the actual distribution of diffuse light from Lambertian and this influence on the solar sail thrust calculation. Lambertian diffuse reflection states that light is uniformly scattered around the reflection point (see Fig. 3). The non-Lambertian coefficient models the non-uniform diffuse reflection of light off a near specular surface.

By inspection of the reported values in Refs. [1-3], the backside non-Lambertian coefficient appears to be consistently set equal to the back side emissivity coefficient. Although we have not definitively identified the source of the back side non-Lambertian coefficient, this is a functional assumption for the time being.

In the next section, we conduct a deeper investigation of the front side non-Lambertian coefficient to derive the origin of the value reported in Ref. [1].

III. Derivation of Non-Lambertian Coefficient

Light, in the form of a single ray, is incident on a flat element of sail material at an angle of attack α . The irradiance on the sail material is $E_i[Wm^{-2}] = P_i/A \cos(\alpha)$, the total power of the incident beam of light $P_i[W]$ impinging the projected surface area of the sail, where $A[m^2]$ is the total area. If we denote $\sigma[m^2]$ as the surface area of a hemisphere placed on the sail and centered on the point of light incidence, then the elementary solid angle of a reflected cone of light, $d\omega$, is given by θ , the angle between the direction of a reflected ray and the surface normal, and ϕ , the clock angle of the reflected ray.

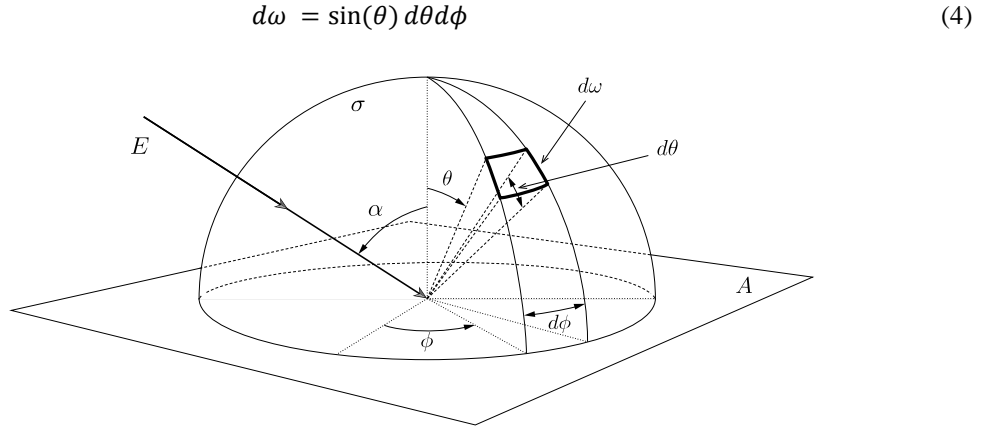


Figure 2. Elementary solid angle of reflected light from a sample flat surface and angular coordinates.

The radiance $L_r[Wm^{-2}sr^{-1}]$, or radiant flux reflected by the sail element within a given solid angle, is

$$L_r = \frac{I_r}{A \cos(\theta)}, \quad (5)$$

the radiant intensity of light reflected in this solid angle, $I_r[Ws^{-1}] = dP_r/d\omega$, over the projected area of the sail onto the direction of the reflected ray, where $P_r[W]$ is the total reflected power in all directions.

The BRDF is defined as the radiance out divided by the irradiance in [11]:

$$BRDF = \frac{L_r}{E_i}[sr^{-1}], \quad (6)$$

or by substitution:

$$BRDF = \frac{dP_r/d\omega}{P_i \cos(\theta)}. \quad (7)$$

If, for the sake of simplicity, we ignore the any absorption (and thus any re-radiance) of the sail material, then from the conservation of momentum, we can write the normal force (Eq. 2) on the sail in terms of incident and reflected power:

$$F_n = \frac{P_i}{c} \cos(\alpha) + \int_{\sigma} \frac{dP_r}{c}, \quad (8)$$

where c is the speed of light in vacuum. Using the expression for BRDF (Eq. 7) and replacing the incident power with irradiance and area, we rewrite this force:

$$F_n = \frac{E_i A}{c} \left[\cos^2(\alpha) + \cos(\alpha) \int_{\sigma} BRDF \cos(\theta) d\omega \right] \quad (9)$$

As discussed earlier, light reflected off a surface is generally expressed in two components: specular and diffuse. Mathematically, we express the specular component as a delta function, denoted $\delta(\cdot)$, in the direction of $\theta = \alpha$. The diffuse component, on the other hand, is some amplitude function over the hemisphere σ . We denote this as $f_d(\theta, \phi)$. A priori, integration of the specular component of reflected light must have a maximum value equal to $\tilde{\mathbf{r}}\mathbf{s}$. Similarly, all other reflected light, which is diffuse, must maximally equal $\tilde{\mathbf{r}}(1 - \mathbf{s})$. Therefore, we normalize these reflectance distributions in the force equation [12]:

$$F_n = \frac{E_i A}{c} \left[\cos^2(\alpha) + \tilde{\mathbf{r}}\mathbf{s} \cos(\alpha) \frac{\int_{\sigma} \delta(\theta - \alpha) \delta(\phi) \cos(\theta) d\omega}{\int_{\sigma} \delta(\theta - \alpha) \delta(\phi) d\omega} + \tilde{\mathbf{r}}(1 - \mathbf{s}) \cos(\alpha) \frac{\int_{\sigma} f_d(\theta, \phi) \cos(\theta) d\omega}{\int_{\sigma} f_d(\theta, \phi) d\omega} \right], \quad (10)$$

where

$$\frac{\int_{\sigma} \delta(\theta - \alpha) \delta(\phi) \cos(\theta) d\omega}{\int_{\sigma} \delta(\theta - \alpha) \delta(\phi) d\omega} = \cos(\alpha) \quad (11)$$

and

$$\frac{\int_{\sigma} f_d(\theta, \phi) \cos(\theta) d\omega}{\int_{\sigma} f_d(\theta, \phi) d\omega} = \mathbf{B}_f, \quad (12)$$

is the non-Lambertian coefficient so that Eq. 10 now looks like Eq. 2 if emissivity is excluded.

With this expression for the non-Lambertian coefficient, we can now study this coefficient further. Say a sail material is a perfect Lambertian surface. By definition, the BRDF must be uniform over the hemisphere, σ , such that

$$f_d(\theta, \phi) = \cos(\theta) 1(\phi). \quad (13)$$

Therefore, the non-Lambertian coefficient for a Lambertian surface from Eq. 12 is

$$\mathbf{B}_f = \frac{\int_{\phi=0}^{2\pi} \int_{\theta=0}^{\pi/2} \cos^2(\theta) \sin(\theta) d\theta d\phi}{\int_{\phi=0}^{2\pi} \int_{\theta=0}^{\pi/2} \cos(\theta) \sin(\theta) d\theta d\phi} = \frac{2}{3}, \quad (14)$$

a value also reported by many [2-3,12].

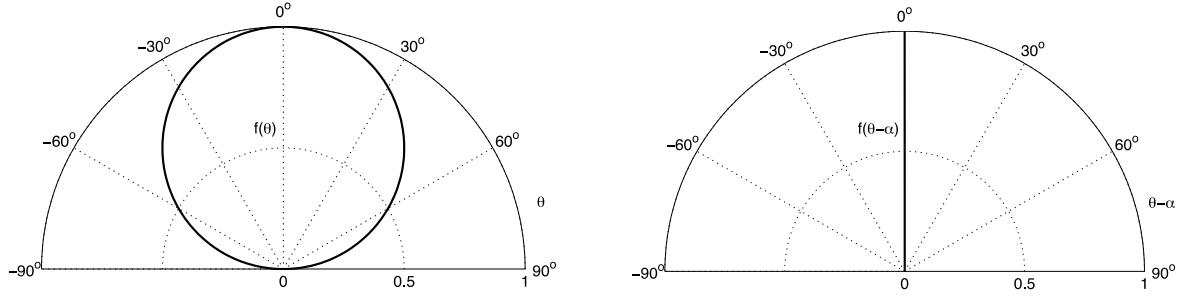


Figure 3. (left) Reflectance distribution for a perfect Lambertian surface. (right) Reflectance distribution for a perfectly specular surface.

Using Eq. 12, the authors calculated the front surface non-Lambertian coefficient from two sets of BRDF data of solar sail material: 1) pristine aluminized Kapton illuminated at 10 deg incidence reported in the 1978 JPL report [1], and 2) wrinkled aluminized Mylar illuminated at 25 deg incidence collected in 2006 by B. Derbes [9]. Assuming a specular cone of 10 deg for both datasets, numerical integration over only the diffusely reflected light returned \mathbf{B}_f values of 0.79 and 0.86 for the Kapton and Mylar data sets, respectively. If, however, for the wrinkled Mylar data set we define the specular cone as 20° since the specular peak in this data set is wide, then the non-Lambertian coefficient equals 0.79. The value published in the 1978 JPL report for \mathbf{B}_f appears to be reasonable given that the material tested in that case was highly specular and under considerable tension. What is more, this corroboration of reported data directs us to the appropriate method for determining \mathbf{B}_f values of new sail materials from future BRDF measurements.

IV. Updated Optical Coefficients

The optical coefficients have been updated for NEA Scout and Lunar Flashlight with the exception of s , the fraction of reflection that is not specular, and \mathbf{B}_f , the non-Lambertian coefficient. These two exceptions will be updated following future testing of crinkled and wrinkled sail material under tension appropriate to the particular mission. The existing data from [1] is sufficient for a highly tensioned “pristine” (i.e. non-wrinkled) sample, and, until new data is collected, these values will continue to be assumed as nominal. All other coefficients in the solar sail thrust model have been updated with descriptions, which follow.

The updated value of \tilde{r} (total reflectivity) is based on optical testing conducted at the Marshall Space Flight Center (MSFC) in 2004 [10]. This testing found the total reflectivity of CP1 coated with 100 nm of AL to be 0.91. Above, we quote a section from the JPL report, NASA-CR-157870, indicating that in 1978 the value of 0.88 was selected because it was at the lower end of a range measured from 0.88 to 0.91. The 2004 test at MSFC had a one-sigma deviation of 0.005. Thus we update this coefficient to be 0.91 ± 0.005 .

Solid data on front and back side emissivity of the AL-coated CP1 was also collected in the 2004 MSFC tests. We note that the emissivities will vary dramatically from what is reported in Table 1, since the 1978 test used Kapton that was also back side coated in chromium. For the front side emissivity, the 2004 MSFC test determined the value to be 0.025 ± 0.005 . The uncoated back side emissivity of 2.5 micrometer CP1 is 0.27 ± 0.005 – a significant deviation from 0.55 determined for back side chromium coated Kapton. It should be stressed that these updated emissivity values are applicable only to 2.5 micrometer CP1 coated with 100 nm of AL on the front side with an uncoated back side. Other sail materials – for instance the 5 micrometer Mylar being used on the Planetary Society LightSail-A and LightSail-B [13] – will have different emissivity values and must be determined from appropriate testing.

Discussed earlier, we believe the value of \mathbf{B}_b , the back side non-Lambertian coefficient, was set to be the same value as the back side emissivity coefficient. There does not appear to be any test data to support this assumption. We choose not to follow that precedent. In the absence of any test data from the 2004 test for this parameter, we assign it the ideal value of 0.67 (the value for a Lambertian distribution). There are no current plans to perform testing on this parameter since its effect on thrust is incredibly small. Even if the distributed radiation from the back side of the sail varies greatly from a Lambertian distribution, the effect on thrust will be minimal.

Coefficient	\tilde{r}	s	B_r	B_b	e_r	e_b
Value	0.91	0.94	0.79	0.67	0.025	0.27
	+/-0.005	+/-0.04	+/-0.05	+/-0.05	+/-0.005	+/-0.005

Table 3. Updated optical coefficients for NEA Scout and Lunar Flashlight missions

Presented in Table 3, we update three of the six optical parameters in the standard NASA model of solar sail thrust for AL coated, 2.5 micrometer CP1. Updates to s and B_r are forthcoming following additional testing, while B_b is assumed to reflect an ideal Lambertian distribution. Table 3 lists the updated model optical coefficients and includes their approximate uncertainty. The uncertainties for \tilde{r} , e_r , and e_b are based on optical testing conducted at MSFC in 2004 [10]. The uncertainty in s is based on a discussion of that parameter in Ref. [1]. The uncertainty in B_b is assumed to be the same as the uncertainty in B_r since these two parameters are similar, and both are based solely on engineering judgment, since adequate test data to determine uncertainty does not yet exist.

V. Recent Developments

In 2014, new tests of reflectivity for modern solar sail designs were conducted at MSFC to support the reflectivity requirement of the Lunar Flashlight mission. This requirement places a minimum value on the amount of light that is reflected off the sail toward the lunar surface within a 3 deg. cone of the normal axis of the sail. The exact amount of light to be reflected is currently subject to revision.

The Lunar Flashlight requirement is similar to how diffusivity is typically determined (i.e., light reflected within a certain cone of the specular reflection ray). In the case of the 1978 testing as discussed above, light was measured in a cone of 10 deg, and anything outside that cone was considered diffuse. There is, however, a difference between the Lunar Flashlight reflectivity testing and a typical diffusivity test. A standard BRDF diffusivity test uses a point illumination so the measurements are indications only of what happens at the microscopic scale (i.e. on the order of a micrometer).

In contrast to a typical diffusivity test, the Lunar Flashlight reflectivity requirement also mandates knowledge of reflective properties at the “meso” (on the order of millimeters) and “macro” (or the order of meters) scales. The mesoscale level would be affected by factors such as wrinkles, folds, and the presence of rip stop in the sail material. The macroscale level would be affected by factors such as boom deflection, sail membrane shape, and manufacturing tolerances on the sail.

The microscale influences on sail reflectivity can be well determined by point-based BRDF and similar tests while the macroscale influences can be determined from computer and analytical models. The mesoscale influences are more difficult both to measure and model and so there is a gap in knowledge in this area.

The mesoscale reflectivity is addressed by measuring reflectance over a specific area of the sail that is significantly larger than a single point. Some testing of this nature was completed recently, although the results are considered inconclusive and additional testing is underway at the time of publication of this paper. The test setup from the first round of testing, performed in 2014 and aiming to determine mesoscale reflectivity influences, appears in Fig. 4.



Figure 4. Mesoscale reflectivity test apparatus

The test article, a sheet of AL coated CP1 sail material, appears on the right side of Fig. 4. This particular test article, at 1 meter along each diagonal edge, is subscale relative to the NEA Scout and Lunar Flashlight sail designs. The reflectance measurements were collected from a 3 deg cone of reflected light incident on the sail at 45 deg while a ~10 cm region of the sail was illuminated. Eighteen regions of the sail sample were illuminated, and a reflectance calculated for each region, see Fig. 5. The tension of the sail was controlled and reflectance measurements were conducted at levels of tension encompassing mission expectations, scaled according to the reduced size of the test sail. The sail was also stored as it would be prior to flight in order to simulate realistic folds and wrinkles to accurately capture mesoscale effects on reflectivity.

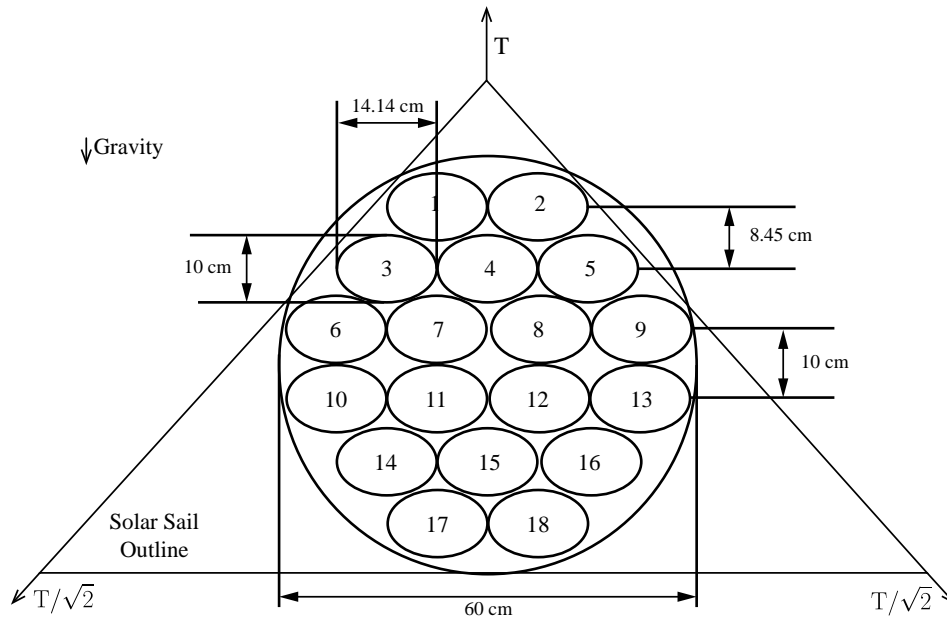


Figure 5. August 2014 areal measurements of 18 regions of a subscale sail sample while varying tension (T) applied to the vertices all to determine mesoscale reflectivity.

The results of this 2014 testing were inconclusive and additional tests are now scheduled for August of 2015 (around the time of this paper's presentation and publication). The new 2015 tests differ slightly in that smaller test articles, called coupons, will be used for the tests. These coupons will be easier to subject to the proper tension while being capable of capturing all the mesoscale effects. A depiction of a single coupon appears in Fig. 6.

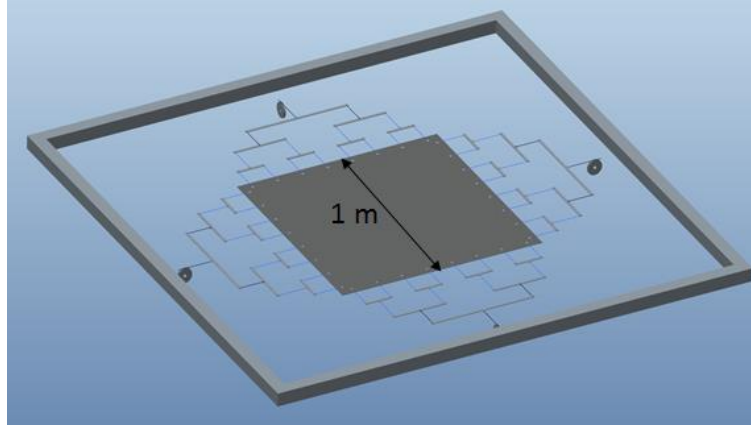


Figure 6. Test Coupon for August 2015 Optical Test

The test coupon is 1 square meter. Tension is distributed across the square meter much more uniformly than was possible in the 2014 tests. The results of this testing will primarily be used to determine if Lunar Flashlight can meet its reflectivity requirement, yet they will also be useful for further updates to the thrust model.

Currently we are analyzing the shape of the updated single membrane sail design. Until recently, NEA Scout and Lunar Flashlight were using a quadrant design for the sail. With the quadrant design, the booms of the sail were exposed to large thermal gradients, which caused unacceptably large deformations across the sail. Thus, the current design consists of a single membrane that shades the booms from the sun, ensuring a small thermal gradient across the boom.

We are just beginning to analyze the effects of this single membrane shape on sail thrust given its departure from a flat plate. Preliminary results suggest that the primary effect of the departure from flatness is a reduction in thrust on the order of 4% while the thrust direction varies less than 0.1 degrees. An angular offset this small allows us to treat the membrane model as a flat plate with a reduction in area. However, current plans call for NEA Scout and Lunar Flashlight to use a lookup table for thrust from preliminary calculations based on a shape simulated from structural and thermal models. This model will then be calibrated during the mission. The simulated thrust will use the same optical model discussed in this paper for the elements of the shape model, and this update is critical to ensure mission success.

VI. Conclusions and Future Work

The sources of the optical thrust model coefficients that NASA has typically used to estimate sail performance have been reviewed and revised. Four of the coefficients - \tilde{r} , s , e_f , and e_b - have a clear derivation from [1]. The derivation of B_f and B_b from that source is not clear, and that for B_b appears to be unavailable. We performed an analysis of B_f using the reported BRDF data in [1] and in [9] and found the regularly used value of 0.79 to be acceptable for pristine sails. There is no information at all available for the original derivation of B_b , though it may have been assumed to be the same as e_b since it is only used for the re-radiation force on the unlit side of the sail. Since B_b has only a small effect on the thrust model, knowledge of its original derivation is not critical.

We update four of the optical coefficients using test data from 2004. This update is primarily intended to support NEA Scout and Lunar Flashlight - 100 nm AL coated 2.5 micrometer CP1 with an uncoated back side. Due to the opaque optical thickness of the AL coating, the reported coefficients relating to reflectance characteristics will apply to any AL coated sail material, whereas the emissivity coefficients are material specific and would not apply to back side coated sails or sails made of Kapton or Mylar. The values of \tilde{r} , e_f , and e_b have been updated with a small residual uncertainty. The values of s and B_f will be updated when optical testing concludes in late 2015. The value of B_b has a very small effect on the thrust model and currently there are no plans to conduct any tests to refine its value. We assume B_b has the ideal value of 0.67 corresponding to Lambertian distributed radiation on the backside of the sail.

These new values for the solar sail thrust model optical coefficients are in support of the current NASA solar sail missions – NEA Scout and Lunar Flashlight. Both missions will rely heavily on thrust predictions from the sail model. These updates are, therefore, critical to the success of these missions.

References

1. NASA-CR-157870 “Sail Materials and Supporting Structure for a Solar Sail, a Preliminary Design”, Volume 4, Jet Propulsion Laboratory, Pasadena, CA, 1978.
2. Wright, J. L., *Space Sailing*, Gordon and Breach Science Publishers, 1992.
3. McInnes, C. R., *Solar Sailing: Technology, Dynamics, and Mission Applications*, Springer-Praxis Series in Space Science and Technology, Springer-Praxis, Chichester, UK, 1999.
4. Wie, B., “Dynamic Modeling and Attitude Control of Solar Sail Spacecraft”, NASA Solar Sail Technology Working Group (SSTWG) Final Report Jan. 10, 2002.
5. Heaton, A.F., Faller, B.F., and Katan, C.K., “NanoSail-D Attitude and Orbital Dynamics”, 2nd International Symposium on Solar Sailing, Glasgow, Scotland, 2012.
6. Braafladt, Alexander, Artusio-Glimpse, Alexandra, and Heaton, Andrew, “Validation of Solar Sail Simulations for the NASA Solar Sail Demonstration Project”, AIAA SPACE 2014 Conference, San Diego, August 2014.
7. McNutt, L., et al, “The Near Earth Asteroid Scout”, AIAA SPACE 2014 Conference, San Diego, CA, August 2104.
8. Nicodemus, Fred, “Directional Reflectance and Emissivity of an Opaque Surface”, Applied Optics, Vol. 4, No. 7, ppg 776-773, July 1965.
9. Derbes, Billy, and Lichodziejewski, David, “Propulsive Reflectivity and Photoflexibility: Effects on Solar Sail Performance and Control”, AIAA/ASME/SAE/ASEE Joint Propulsion Conference, Sacramento, CA, July 2006.
10. Nehls, M., “CP1 Environmental Effects Testing”, NASA MSFC Technical Report, September 2005.
11. Papetti, T., Walker, W., Keffer, C., and Johnson, B., “MRDF and BRDF measurements of low-scatter materials,” Proc. SPIE 6550, Laser Radar Technology and Applications XII, 65500H, May 2007.
12. Georgevic, R. M. “Mathematical Model of the Solar Radiation Force and Torques Acting on the Components of a Spacecraft”, NASA Technical Memorandum 33-494, Jet Propulsion Laboratory, October 1971.
13. Johnson, L., Alhorn, D., Boudreaux, M., Casas, J., Stetson, D., Young, R., “Solar and Drag Sail Propulsion: From Theory to Mission Implementation,” AIAA Space Propulsion, May 2014.